

Article

A Microsomal Proteomics View of H₂O₂- and ABA-Dependent Responses

May Alqurashi ^{1,2,†}, Ludivine Thomas ^{3,†}, Chris Gehring ^{2,4}  and
Claudius Marondedze ^{1,2,5,*} 

¹ Cambridge Centre for Proteomics, Cambridge Systems Biology Centre, Department of Biochemistry, University of Cambridge Tennis Court Road, Cambridge CB2 1QR, UK; may.qurashi@kaust.edu.sa

² Biological and Environmental Sciences & Engineering Division, King Abdullah University of Science and Technology, Thuwal 23955-6900, Saudi Arabia; c.a.gehring@molecular-signals.com

³ HM. Clause, rue Louis Saillant, Z.I. La Motte, BP83, 26802 Portes-lès-Valence, France; ludivinet1@gmail.com

⁴ Department of Chemistry, Biology & Biotechnology, University of Perugia, Borgo XX giugno 74, 06121 Perugia, Italy

⁵ Laboratoire de Physiologie Cellulaire et Végétale, Université Grenoble Alpes, CEA/BIG, 17, avenue des Martyrs, 38054 Grenoble, France

* Correspondence: cmarondedze@gmail.com or cm833@cam.ac.uk; Tel.: +33-427-680-479

† These authors contributed equally to this work.

Received: 18 May 2017; Accepted: 16 August 2017; Published: 18 August 2017

Abstract: The plant hormone abscisic acid (ABA) modulates a number of plant developmental processes and responses to stress. In planta, ABA has been shown to induce reactive oxygen species (ROS) production through the action of plasma membrane-associated nicotinamide adenine dinucleotide phosphate (NADPH)-oxidases. Although quantitative proteomics studies have been performed to identify ABA- or hydrogen peroxide (H₂O₂)-dependent proteins, little is known about the ABA- and H₂O₂-dependent microsomal proteome changes. Here, we examined the effect of 50 μM of either H₂O₂ or ABA on the Arabidopsis microsomal proteome using tandem mass spectrometry and identified 86 specifically H₂O₂-dependent, and 52 specifically ABA-dependent proteins that are differentially expressed. We observed differential accumulation of proteins involved in the tricarboxylic acid (TCA) cycle notably in response to H₂O₂. Of these, aconitase 3 responded to both H₂O₂ and ABA. Additionally, over 30 proteins linked to RNA biology responded significantly to both treatments. Gene ontology categories such as ‘response to stress’ and ‘transport’ were enriched, suggesting that H₂O₂ or ABA directly and/or indirectly cause complex and partly overlapping cellular responses. Data are available via ProteomeXchange with identifier PXD006513.

Keywords: hydrogen peroxide (H₂O₂); abscisic acid (ABA); microsomal proteomics; quantitative proteomics; mass spectrometry

1. Introduction

Plants, much like animals, are susceptible to oxidative damage by reactive oxygen species (ROS). The production of ROS, and in particular hydrogen peroxide (H₂O₂), increases during exposure to abiotic stress [1–3] and pathogen infection [4]. In pathogen infections, suppression of ascorbate peroxidase and catalase during the hypersensitive response enhances pathogen-induced programmed cell death [4]. The mitochondrial electron transport chain also synthesises a significant amount of ROS, mainly in the form of superoxide [5] that can cause oxidative stress [6,7]. Previous studies have shown that the oxidative stress imposed by H₂O₂ is a potent inhibitor of tricarboxylic acid (TCA) cycle enzymes such as citrate synthase [8], aconitase, and succinyl CoA ligase [9–11]. However, at low concentrations, H₂O₂ functions as a stress signal [12,13].

It has been demonstrated that ROS production is required for abscisic acid (ABA) signal transduction in guard cells [14,15]. In the guard cells, ABA is perceived by PYRABACTIN resistance (PYR)/PYR-Like 1/Regulatory components of ABA receptors (RCAR) [16,17], which in turn induce the production of ROS including H₂O₂, by nicotinamide adenine dinucleotide phosphate (NADPH)-oxidase [18,19]. ABA also induces stomatal closure but interestingly, treating the guard cells of ABA-insensitive mutants, *abi1-1*, with ABA did not induce ROS production but activation of hyperpolarised-activated Ca²⁺ (I_{Ca}) channels and the induction of stomatal closure by H₂O₂, suggesting that *abi1-1* disrupts ABA signalling between ABA reception and ROS production [20]. Besides, ABA regulates many plant developmental processes and induces increased tolerance to different stresses such as drought, salinity and low temperature [21]. ABA-induced ROS in the mitochondria of root tip cells operates as retrograde signal that regulate meristem activity in *Arabidopsis* [22]. In maize (*Zea mays*) leaves, water stress-induced ABA accumulation has been detected to elicit an increased production of H₂O₂ [23,24]. Also, in rice (*Oryza sativa*) seedlings, exogenous ABA has been observed to increase H₂O₂ content in leaves grown under potassium sufficient conditions [25].

Despite the considerable body of information on role of ABA in stress responses, the post-translational molecular targets at the microsomal level and particularly their relation with H₂O₂ is yet to be properly understood. Therefore, we set to find out whether H₂O₂ and ABA can induce a common response at the microsomal proteome level. To do this, downstream microsomal protein changes were investigated using label-free quantitative mass spectrometry analysis. Further, to find out whether ABA induces H₂O₂ production or *vice versa*, we tested for H₂O₂ production upon ABA treatment of *Arabidopsis thaliana* ecotype Columbia-0 cell suspension cultures or ABA production upon H₂O₂ treatment. In this study we showed that H₂O₂ and ABA have common and independent responses. The former is however, not surprising, as ABA has previously been shown to induce production of H₂O₂, thus the common response suggests an H₂O₂-dependent response, which can also be elicited via ABA.

2. Materials and Methods

2.1. Treatments of *Arabidopsis* Cell Suspension Culture

Cells derived from *Arabidopsis thaliana* (ecotype Columbia-0) roots were grown in Gamborg's B5 basal salt mixture (Sigma-Aldrich, St. Louis, MO, USA), as described in [26,27]. At Day 7 post-subculturing, three biological replicate flasks containing cells were treated with 50 μM ABA or 50 μM H₂O₂ for 0 min (mock treatment), 5 min and 20 min. Cells were then harvested by draining off the media using a Stericup[®] filter unit (Millipore, Billerica, MA, USA), immediately flash frozen in liquid nitrogen, and stored at −140 °C until further use.

2.2. Microsomal Protein Isolation

Approximately 1 g of cells was ground to a fine powder in liquid nitrogen and subjected to microsomal isolation, as described in [28]. The powder was incubated in a sucrose buffer (50 mM Tris(hydroxymethyl)aminomethane (pH 8.0), 2 mM ethylenediaminetetraacetic acid (EDTA), 2 mM dithiothreitol (DTT), 0.25 M sucrose and 1× protease inhibitor cocktail tablet (Sigma-Aldrich, St. Louis, MO, USA)) and centrifuged at 8000× g for 15 min. The supernatant was subjected to ultracentrifugation using an Optima[™] L-100K ultracentrifuge (Beckman Coulter, Brea, CA, USA) at 100,000× g for 1 h. The supernatant, representing the cytosolic fraction, was pipetted out. The pellet, the microsomal fraction, at the bottom of the tube, was washed once in sucrose buffer and centrifuged at 100,000× g for 1 h. The microsomal fraction corresponding to the final pellet was suspended in sucrose buffer, aliquoted into separate tubes and either used immediately or stored at −80 °C.

2.3. Trypsin Digestion and Protein Identification by Tandem Mass Spectrometry

Approximately 0.2 mg of total microsomal protein extract was reduced with 5 mM DTT for 2 h at 37 °C and cooled. The sample was then alkylated with 14 mM iodoacetamide for 30 min at room temperature in the dark. Unreacted iodoacetamide was quenched by increasing DTT concentration to 10 mM and incubated for 15 min at room temperature in the dark. Proteins were incubated at 50:1 ratio with sequencing-grade modified trypsin (Promega, Madison, WI, USA) overnight at 37 °C with gentle agitation. Protein digestion was stopped by acidification of the mixture to pH 2.0 with trichloroacetic acid. Peptides were desalted using Sep-Pak Vac tC18 100 mg cartridges (Waters, Milford, MA), as described previously [27]. After desalting, peptides were re-suspended in 5% (*v/v*) acetonitrile and 0.1% (*v/v*) formic acid and analysed by the LTQ-Orbitrap Velos mass spectrometer (Thermo-Scientific, Bremen, Germany) coupled with a nano-electrospray ion source (Proxeon Biosystems, Odense, Denmark) for nano-liquid chromatography tandem mass spectrometry (LC-MS/MS) analyses as described in [29]. Five microlitres of the peptide mixtures was injected onto a 50 mm long × 0.3 mm Magic C18AQ (Michrom) column. A spray voltage of 1500 V was applied and the MS scan range used was *m/z* 350 to 1600. The top 10 precursor ions were selected in the MS scan by the Orbitrap with a resolution $r = 60,000$ for fragmentation in the linear ion trap using collision-induced dissociation. Normalised collision-induced dissociation was set at 35.0 and spectra were submitted to a local MASCOT (Matrix Science, London, UK) server and searched against Arabidopsis in the Arabidopsis Information Resource (TAIR, Release 10), with a precursor mass tolerance of 10 ppm, a fragment ion mass tolerance of 0.6 Da, and strict trypsin specificity allowing up to one missed cleavage. Carbamidomethyl modification on cysteine residues was selected as fixed modification, and oxidation of methionine residues as variable modification. Identified proteins were further validated with Scaffold version 4.0.4 (Proteome Software, Portland, OR, USA). Identified proteins were considered positive with a molecular weight search (MOWSE) score ≥ 32 , number of peptides ≥ 2 , a 95% protein and peptide probability, and a false discovery rate (FDR) $\leq 1\%$. Label-free quantitative analysis was performed using spectral counts with Scaffold software. Proteins were deemed responsive to treatment when present in at least two replicates with a fold change (FC) greater or equal to $|\pm 2|$, verified by Student t-test (p -value ≤ 0.05) in comparison to the mock-treated samples. All proteomics methods are extensively detailed elsewhere [26,29–31].

2.4. Intracellular ROS Assay and ABA Measurements

Cellular ROS levels were measured using OxiSelect™ intracellular ROS assay kit green fluorescence (Cambridge Bioscience, Cambridge, UK) after 20 min of 50 μ M ABA treatment. The procedure used was according to the manufacturer's protocol. ABA contents in samples treated with 50 μ M H₂O₂ for 5 and 20 min were measured using Phytodetek® immunoassay kit for ABA (Agdia, Elkhart, IN, USA) according to the manufacturer's instructions.

2.5. Bioinformatic Analyses

The gene ontology (GO) analysis toolkit in the database AgriGO [32] was used for the detection of enriched cellular components, biological processes and molecular functions.

3. Results

To gain insight on the microsomal cellular responses to H₂O₂ and ABA, a comparative proteomic analysis was undertaken. Microsomal proteins were isolated from Arabidopsis cell suspension cultures pre-treated with 50 μ M of either H₂O₂ or ABA for 5 min or 20 min, digested with trypsin and analysed by MS/MS. Data was processed with MASCOT and Scaffold for identification and label-free quantitation. A total of 906 proteins from the enriched samples were identified (Table S1). Of these, 86 proteins were significantly ($p \leq 0.05$) responsive to H₂O₂ treatment (Table 1) and 52 proteins to ABA

treatment (Table 2). A total of 21 responsive proteins were common to both ABA and H₂O₂ treatments and majority of the proteins displayed similar response signatures (Table 3).

Table 1. Proteins responsive to H₂O₂ treatment.

Accession Number	Protein Name	ANOVA (<i>p</i> -Value)	FC 5 min	FC 20 min
1. Metabolism				
AT1G17745	D-3-phosphoglycerate dehydrogenase 2	0.0089	0.1	0.1
AT5G26780	Serine hydroxymethyltransferase 2	0.036	2.1	13
AT3G61440	Cysteine synthase C1	0.00074	ns	5
AT4G14880	O-acetylserine (thiol) lyase isoform A1	0.015	0.1	7.9
AT5G23300	Pyrimidine d	0.013	0.2	ns
AT3G09820	Adenosine kinase 1	0.0042	0.1	14.0
AT5G17770	NADH:cytochrome B5 reductase 1	0.017	0.4	2.5
AT1G74790	Catalytics	0.045	5.7	4.6
AT4G23850	AMP-dep. synthetase and ligase protein	0.017	0.5	ns
AT1G65290	Mitochondrial acyl carrier protein 2	0.044	2.9	ns
AT3G47930	L-galactono-1,4-lactone dehydrogenase	0.019	0.2	ns
2. Energy				
AT1G79550	Phosphoglycerate kinase	0.0069	0.2	2.0
AT1G24180	Pyruvate dehydrogenase E1 comp. α -2	0.014	0.1	0.2
AT3G48000	Aldehyde dehydrogenase 2B4	0.022	4.3	7.1
AT3G60750	Transketolase	0.0087	0.5	4.5
AT2G05710	Aconitase 3	0.0002	2.5	12.0
AT2G20420	ATP citrate lyase	0.022	ns	5.0
AT5G08300	Succinyl-CoA ligase, alpha subunit	0.006	2.4	2.5
AT2G44350	Citrate synthase family protein	0.026	ns	5.9
AT1G65930	Cyt. NADP ⁺ -dep. isocitrate dehydrogenase	0.033	0.1	2.9
AT1G15120	Ubiquinol-cytochrome C reductase hinge	0.016	19	20
AT3G03100	NADH:ubiquinone oxidoreductase, 17.2kDa	0.0029	0.5	ns
AT5G13430	Ubiquinol-cytochrome C reductase, Fe-S	0.02	0.2	ns
AT3G14610	Cytochrome P450, 72A, polypeptide 7	0.0026	0.1	5.4
3. Cell growth/division				
AT5G52240	Membrane steroid binding protein 1	0.02	0.1	7.5
AT1G10930	DNA helicase (RECQ14A)	0.0036	4.6	0.1
AT3G44310	Nitrilase 1	0.023	2.9	ns
4. Transcription				
AT1G14850	Nucleoporin 155	0.00094	ns	0.3
5. Protein synthesis				
AT1G01100	60S acidic ribosomal	0.022	ns	0.4
AT3G48930	Nucleic acid-binding, OB-fold-like protein	0.024	2.1	ns
AT3G10090	Nucleic acid-binding, OB-fold-like protein	0.027	ns	0.3
AT3G09200	Ribosomal protein L10	0.012	2.9	ns
AT3G04400	Ribosomal protein L14p/L23e	0.0095	3.8	3.0
AT1G23290	Ribosomal protein L18e/L15	0.017	ns	0.5
AT4G02230	Ribosomal protein L19e	0.0089	ns	0.3
AT2G44120	Ribosomal protein L30/L7	0.027	ns	0.5
AT5G56710	Ribosomal protein L31e	0.013	4.6	ns
AT3G45030	Ribosomal protein S10p/S20e	0.03	ns	2.2
AT5G02960	Ribosomal protein S12/S23	0.016	2.3	ns
AT3G60245	Zinc-binding ribosomal protein	0.036	2.4	ns
6. Protein destination and storage				
AT1G14980	Chaperonin 10	0.022	ns	2.9
AT3G02530	Chaperonin 60 family protein	0.045	2.2	0.4
AT3G03960	Chaperonin 60 family protein	0.041	2.1	ns
AT5G56030	Heat shock protein 81-2	0.012	0.4	ns
AT3G52140	Tetratricopeptide repeat-containing protein	0.04	5.3	ns
7. Transporters				
AT4G38580	Farnesylated protein 6	0.017	0.4	ns
AT3G15660	Glutaredoxin 4	0.011	ns	6.0
AT1G27950	Glycosylphosphatidylinositol-anchored lipid protein transfer 1	0.027	16.0	44.0
AT1G07670	Endomembrane-type CA-ATPase 4	0.0026	0.1	5.0
AT4G27500	Proton pump interactor 1	0.006	ns	2.4
AT4G39080	Vacuolar proton ATPase A3	0.0041	0.5	ns
AT3G58730	Vacuolar proton pump D subunit	0.044	0.4	ns
AT1G15500	TLC ATP/ADP transporter	0.0099	0.3	ns

Table 1. Cont.

Accession Number	Protein Name	ANOVA (<i>p</i> -Value)	FC 5 min	FC 20 min
1. Metabolism				
AT4G28390	ADP/ATP carrier 3	0.014	0.1	ns
AT5G60460	Preprotein translocase Sec, Sec61- β subunit	0.0081	4.7	4
AT3G51890	Clathrin light chain protein	0.019	ns	0.5
AT3G08530	Clathrin, heavy chain	0.0021	0.5	0.2
AT3G11130	Clathrin, heavy chain	0.00044	0.5	0.4
AT5G19760	Mitochondrial substrate carrier protein	0.038	ns	2.2
AT5G40810	Cytochrome C1	0.021	0.3	ns
8. Intracellular traffic				
AT3G49560	Mit. import inner membrane translocase Tim17	0.0031	0.1	ns
AT1G61570	Mit. import inner membrane translocase 13	0.0044	17	23
AT1G27390	Translocase outer membrane 20-2	0.0015	0.1	2.1
AT3G60600	Vesicle associated protein	0.051	ns	3
AT4G34660	SH3 domain-containing protein	0.039	4.7	ns
9. Cell structure				
AT5G09810	Actin 7	0.0038	0.5	ns
AT5G19770	Tubulin alpha-3	0.016	0.1	ns
AT5G62690	Tubulin beta chain 2	0.006	0.4	0.4
AT2G29550	Tubulin beta-7 chain	0.0034	0.3	0.4
AT4G14960	Tubulin/FtsZ family protein	0.036	0.4	0.5
AT3G08950	Electron transport SCO1/SenC protein	0.045	0.1	4.3
10. Signal transduction				
AT3G14840	LRR transmembrane protein kinase	0.025	ns	11
AT5G59840	Ras-related small GTP-binding protein	0.0084	0.1	2.7
AT3G51800	Metalloproteinase M24	0.0015	5.1	ns
11. Disease/Defence				
AT3G57280	Transmembrane proteins 14C	0.014	0.1	ns
AT3G12500	Basic chitinase	0.035	ns	2.1
AT3G32980	Peroxidase superfamily protein	0.012	ns	3
AT4G36430	Peroxidase superfamily protein	0.015	0.1	ns
12. Unclassified				
AT2G40765	Unknown protein	0.019	2	ns
AT2G46540	Unknown protein	0.033	ns	3.5
AT4G12590	Transmembrane protein, DUF106	0.033	0.3	ns
AT1G08480	Unknown protein	0.048	0.2	0.4
AT3G20370	TRAF-like family protein	0.0058	0.2	3
AT3G49720	Unknown protein	0.016	0.1	0.3
AT4G24330	DUF1682, unknown protein	0.0077	0.1	2.2
AT2G33585	Unknown protein	0.019	0.1	13

Notes: no significant change against the mock treated samples; dep.: dependent; comp.: component; cyt.: cytosolic; ANOVA: Analysis Of Variance.

Table 2. Proteins responsive to abscisic acid (ABA) treatment.

Accession Number	Protein Name	ANOVA (<i>p</i> -Value)	FC 5 min	FC 20 min
1. Metabolism				
AT2G26400	Acireductone dioxygenase 3	0.035	3.9	6.8
AT4G34200	D-3-phosphoglycerate dehydrogenase 1	0.017	0.5	ns
AT1G17745	D-3-phosphoglycerate dehydrogenase 2	0.029	0.1	0.2
AT4G13940	S-adenosyl-L-homocysteine hydrolase	0.028	2.5	2.0
AT3G17820	Glutamine synthetase 1.3	0.023	3.7	3.5
AT5G17770	NADH cytochrome B5 reductase 1	0.046	2.3	2.3
AT3G15730	Phospholipase D α 1	0.014	3.2	3.8
2. Energy				
AT2G01140	Aldolase superfamily protein	0.0075	5.0	5.1
AT5G43940	GroES-like zinc-binding dehydrogenase	0.014	4.5	5.2
AT4G34870	Rotamase cyclophilin 5	0.0015	3.1	2.7
AT2G05710	Aconitase 3	0.035	8.0	9.9
AT1G15120	Ubiquinol-cytochrome C reductase hinge	0.041	15.0	11.0
AT2G33220	GRIM-19 protein	0.017	2.9	7.1
3. Cell growth/division				
AT5G43070	WPP domain protein 1	0.042	0.4	0.2

Table 2. Cont.

Accession Number	Protein Name	ANOVA (<i>p</i> -Value)	FC 5 min	FC 20 min
1. Metabolism				
4. Transcription				
AT2G18740	Small nuclear ribonucleoprotein	0.02	7.7	4.3
AT5G40480	Embryo defective 3012	0.0084	5.6	7.9
AT1G14850	Nucleoporin 155	0.0058	0.1	0.2
5. Protein synthesis				
AT1G08360	Ribosomal protein L1p/L10e	0.037	3.1	ns
AT4G10450	Ribosomal protein L6	0.00092	12.0	>0.1
AT5G08180	Ribosomal protein L7Ae	0.022	11.0	8.7
AT3G04400	Ribosomal protein L14p	0.016	3.5	2.6
AT3G14600	Ribosomal protein L18ae	0.033	3.4	3.3
AT3G45030	Ribosomal protein S10p/S20e	0.0041	2.3	ns
AT5G47930	Zinc-binding ribosomal protein	0.027	8.6	7.0
AT4G00810	60S acidic ribosomal protein family	0.042	0.4	0.4
AT1G01100	60S acidic ribosomal protein family	0.045	0.4	0.4
AT5G47700	60S acidic ribosomal protein family	0.0085	0.3	0.4
6. Protein destination and storage				
AT1G14980	Chaperonin 10	0.0061	2.5	3.0
AT3G16420	PYK10-binding protein 1	0.017	0.3	0.5
AT5G56030	Heat shock protein 81-2	0.0038	0.4	0.5
AT1G03220	Eukaryotic aspartyl protease	0.0045	2.3	2.5
7. Transporters				
AT3G53420	Plasma membrane intrinsic protein 2A	0.031	0.3	ns
AT3G42050	Vacuolar ATP synthase subunit H	0.045	4.4	4.2
AT4G27500	Proton pump interactor 1	0.0048	ns	2.3
AT2G34250	SecY protein transport	0.011	2.5	3.9
AT3G08530	Clathrin, heavy chain	0.0019	0.2	0.4
AT3G11130	Clathrin, heavy chain	0.00054	0.3	0.4
8. Intracellular traffic				
AT2G29530	TIM10 zinc finger protein	0.021	6.0	5.0
AT1G61570	Mit. import inner membrane 13 translocase	0.042	19.0	11.0
9. Cell structure				
AT4G30270	Xyloglucan endotransglucosylase	0.045	ns	3.0
AT3G18780	Actin 2	0.016	0.3	ns
AT5G09810	Actin 7	0.00073	0.5	0.5
AT5G19770	Tubulin alpha-3	0.044	0.5	0.3
AT5G62690	Tubulin beta chain 2	0.003	0.3	0.4
AT2G29550	Tubulin beta-7 chain	0.0072	0.3	0.4
AT4G14960	Tubulin/FtsZ family protein	0.019	0.4	0.3
10. Signal transduction				
AT3G14840	LRR transmembrane protein kinase	0.014	8.3	14.0
AT3G51800	Metallopeptidase M24	0.027	3.4	ns
11. Disease/Defence				
AT1G78850	D-mannose binding lectin protein	0.0013	14.0	18.0
AT2G43610	Chitinase family protein	0.05	ns	0.3
AT4G38740	Rotamase CYP 1	0.02	2.6	ns
AT1G20620	Catalase 3	0.0064	3.5	2.1

Notes: no significant change against the mock treated samples.

3.1. H₂O₂-Responsive Microsomal Proteins

Of the 86 H₂O₂-dependent significantly changing proteins, 24 proteins increased and 42 proteins decreased in abundance at 5 min, while, 38 proteins increased and 18 proteins decreased in abundance at 20 min. These proteins were classified into 12 major functional categories [31] (Table 1, in depth detail in Table S2). The most represented functional categories include transporters (17%), energy (15%) and protein synthesis (14%) (Table 1). Gene ontology (GO) analysis of the H₂O₂ responsive proteins revealed enrichment in biological processes such as 'cellular process', 'metabolic process', 'response to stress' and 'transport' (Table S2). In addition, enriched molecular function categories included 'structural molecule activity', 'transporter activity' and 'oxidoreductase activity' (Table S2).

Further, we performed metabolic pathway analyses using the Kyoto Encyclopedia of Genes and Genomes (KEGG) database to find out if any pathways were represented. The 'purine metabolism' (13 proteins), 'thiamine biosynthesis' (11 proteins), and 'citrate cycle (TCA cycle)' (six proteins) (Table S2) were the most represented. The abundance of five of the six proteins associated with the TCA cycle increased, particularly at 20 min after H₂O₂ treatment (Figure 1). The responsive proteins included pyruvate dehydrogenase (AT1G24180), an essential precursor that links glycolysis to the TCA cycle, citrate synthase (AT2G44350), aconitase 3 (AT2G05710), isocitrate dehydrogenase (AT1G65930), succinyl-CoA ligase, alpha subunit (AT5G08300), and ATP citrate lyase/succinyl-CoA synthetase (AT2G20420), an enzyme that cleaves citrate to oxaloacetate and acetyl CoA in the presence of ATP and CoA, and is implicated in carbohydrate metabolism and production of fatty acids (Table 1; Figure 1). Citrate synthase catalyses the first committed step in the TCA cycle, and has been shown to decrease in activity by 54% upon oxidation by H₂O₂ [8]. Site-directed mutagenesis of six cysteine residues of citrate synthase showed that the mutant proteins could convert acetyl CoA to oxaloacetate with decreased efficiencies compared to the unmodified citrate synthase. The Cys108Ser and Cys325Ser had their activities decreased by 98%, suggesting that the Cys108 and Cys325 are important for citrate synthase activity. These two nearly inactive forms showed high insensitivity to H₂O₂, while other mutants just like the unmodified citrate synthase had decreased activities upon H₂O₂ treatment [8]. Similar to the observed change in citrate synthase upon H₂O₂ treatment [8], we observed citrate synthase together with pyruvate dehydrogenase significantly decreasing in abundance, particularly 20 min after treatment. Furthermore, it has been shown that pyruvate dehydrogenase and the TCA enzymes, including citrate synthase and aconitase, are sensitive to H₂O₂ [9]. Of these, aconitase is the most sensitive to the H₂O₂ effect [9]. Aconitase is one of the five enzymes that exerted the most influence on controlling the TCA, with a control coefficient of 0.964 (the control coefficient is the measure of the ratio of relative change in flux and the relative change in enzyme amount [33]), the second highest after malate dehydrogenase (1.76) [34]. Other enzymes identified that changed in response to H₂O₂ had a lower control coefficient; for example citrate synthase −0.4, isocitrate dehydrogenase −0.123 and succinyl CoA ligase 0.0008 [34]. Aconitase converts citrate to isocitrate and contains a Fe-S cluster that is one of the primary target sites for ROS effect [35]. In animals, aconitase activity is suppressed by treatment with 50 μM H₂O₂, that in turn causes reduced TCA cycle activity in the cardiac cells [36]. In plants, aconitase affects superoxide dismutase transcription, and has been implicated in regulating resistance to oxidative stress, cell death and salt stress in *Arabidopsis* and *Nicotiana benthamiana* [37]. This phenomenal role of aconitase in regulating oxidative stress was also supported by our data, in which the abundance of aconitase increased in response to H₂O₂ as well as ABA (Table 2). The latter may have been an ABA-dependent response or potentially an ABA-dependent H₂O₂ response. Aconitase has also been observed to increase in abundance in response to cyclic guanosine 3', 5'-monophosphate (cGMP), a second messenger that also showed a time- and concentration-dependent ROS production [28]. It is important to note that the observed increase in aconitase 3 did not necessarily reflect an increase in its activity that consequently could lead to a TCA flux. This is so because it has been shown that aconitase activity is strongly reduced by H₂O₂ [9–11]. Rather, the increase may have been channelled towards its role as RNA-binding protein, where it regulates transcription and stability of mRNA transcripts, including its own [38,39]. Besides, the role of aconitase in RNA-binding and oxidative stress requires further analysis. Overall, a total of 36 H₂O₂-responsive proteins were experimentally linked to potential RNA interaction, including the other TCA cycle enzymes, isocitrate dehydrogenase, succinyl CoA ligase, and succinyl CoA synthase, that increased in abundance at 20 min post H₂O₂ treatment [39]. Taken together, an increase in the aconitase in response to ABA, cGMP or H₂O₂ may suggest a potential role of these signalling molecules in modulating oxidative stress as well as energy supplies.

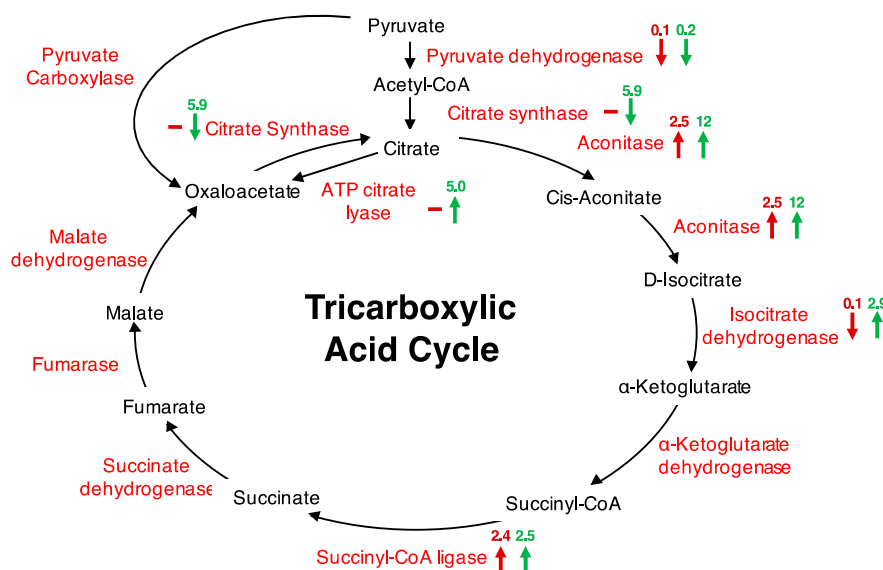


Figure 1. Tricarboxylic acid (TCA) cycle highlighted proteins changing in abundance after H₂O₂ treatment of cells. Maroon arrows represent proteins changing at 5 min after treatment and green arrows at 20 min after treatment. “–” signifies no change or a change of less than two-fold, “↑” signifies an increase in abundance, and “↓” signifies a decrease in abundance. Respective protein fold changes are indicated on top of each arrow.

3.2. ABA-Responsive Microsomal Proteins

A total of 52 proteins showed differential accumulation in response to ABA and 26 of these proteins have been identified as either RNA-binding proteins or candidate RNA interactors [39]. Abundance of 31 proteins increased and 18 decreased at 5 min after treatment with ABA, while at 20 min, 28 proteins increased and 17 proteins decreased (Table 2). The 52 proteins were classified into 11 functional categories [31], and the most represented functional categories were protein synthesis (19%), metabolism (13%), cell structure (13%), and energy (12%) (Table 2; extended summary in Table S3). A functional enrichment analysis of the ABA-responsive proteins revealed significant enrichment of biological processes, including ‘primary metabolic process’, ‘developmental process’, ‘response to stress’, ‘transport’, and ‘translation’ (Table S3). In addition, the molecular functions were also enriched, and these included ‘structural molecule activity’ and ‘transporter activity’ (Table S3). A metabolic pathway analysis was also performed on the ABA-responsive proteins using KEGG, and ‘purine metabolism’ (seven proteins), ‘thiamine metabolism’ (six proteins), and ‘methane metabolism’ (four proteins) were the most represented pathways (Table S3).

Fifteen proteins decreased in abundance at both 5 and 20 min after ABA treatment, and these included six cytoskeleton-associated proteins (Table 2). Three of these were transporter-associated proteins namely clathrin, heavy chains (AT3G08530 and AT3G11130) and a plasma membrane intrinsic protein 2A (PIP2A, AT3G53420). The latter has been linked to other stress-responses, including temperature and salt [40,41], in addition to a potential role in mRNA binding [39]. The abundance of PIP2A, in particular, has been shown to decrease in response to salt stress [41,42], and much like in the current study, the abundance of PIP2A decreased after 5 and 20 min (although at 20 min it was only 0.6 fold change, and hence less than the cutoff of two-fold) of ABA-treatment. PIP2A is a member of the PIP2 subfamily proteins. PIP2A has water transport activity as depicted in *Xenopus laevis* oocytes [43], and facilitates the diffusion of H₂O₂ into cells of yeast [44]. Exposing of Arabidopsis roots to 0.5 mM H₂O₂ has been observed to induce significant depletion of PIP homologs in the plasma membrane fractions after 15 min. In addition, in late endosomal compartments, H₂O₂ has been shown to cause oxidative stress-induced redistribution of *AfPIP2.1* [45]. On another hand, an

ABA-dependent phosphoproteomics analysis detected four members of the aquaporin family including PIP2 decreasing in phosphorylation state at a carboxyl-terminal serine that is anticipated to instigate closure of the water-transporting aquaporin gate [46]. PIP2 dephosphorylation prevents rehydration during ABA-regulated seed germination and dormancy, and decreases water flux in response to drought [46]. Arabidopsis knockout mutants lacking the PIP2:1 aquaporin have a stomatal closure defect particularly in response to ABA [47]. In *pip2:1* plants, ABA treatment induced an increase in osmotic water permeability of guard cell protoplasts while abolishing accumulation of ROS [47], supporting the involvement of aquaporins in ABA-dependent stomatal movements. The work by Grondin et al. [47] implies that PIP2:1 does significantly contribute to guard cell water permeability in the presence of ABA. Moreover, just like Kline et al. [46], Grondin et al. [47] showed that PIP2 phosphorylation is critical for responses to ABA, in particular in guard cell movements. In the current study, differential analysis of microsomal proteins showed that accumulation of PIP2 decreased in the presence of ABA, suggesting a potential direct or indirect regulation of aquaporins in ABA signalling. This may correlate with the decrease in phosphorylation of PIP2 upon ABA treatment [46].

Among the microsomal proteins that increased in abundance after ABA treatment, D-mannose-binding lectin protein (AT1G78850) and LRR transmembrane protein kinase (LTPK, AT3G14840) (Table 2) showed the greatest increase specifically at 20 min. The two proteins play a role in innate immunity against microbial attack. D-mannose-binding lectin recognises certain carbohydrate moieties on pathogen surfaces [48]. It is involved in the regulation of gene expression and cellular activities in response to increasing levels of hormones such as ABA and jasmonate, or biotic and abiotic (e.g., osmotic) stresses [49–53]. On the other hand, LTPK [also known as LYSM RLK1-INTERACTING KINASE 1 (LIK1)], a plasma membrane localised protein, also increased in abundance at 20 min after H₂O₂ treatment. Direct interaction between chitin elicitor receptor kinase (AtCERK1) and LIK1, both in vitro and in vivo studies showed that LIK1 is directly phosphorylated by AtCERK1 [54]. In Arabidopsis, *AtCERK1* mutants show impairment in chitin responses including the activation of a MAPK cascade, ROS production and expression of chitin-induced genes consequently leading to failure of chitin-induced pathogen resistance [55,56]. Furthermore, *Lik1* T-DNA mutant plants produced significantly more ROS in response to chitin and showed an increased resistance to *Pseudomonas syringae* pv. *tomato* [54]. The increase in abundance of LTPK in response to the ABA and H₂O₂ treatments we observed was consistent with the role of LTPK in ROS responses for regulating ROS accumulation that, if in excess, can facilitate necrotrophic infection and promotes programmed cell death [57].

3.3. The Microsomal Proteome of the ABA and H₂O₂ Responses Show Similarity

A total of 21 proteins were common among proteins significantly changing in response to ABA and H₂O₂ treatments. Ten of these proteins have been linked in RNA biology [39]. Changes in abundance for most of these proteins were similar (Table 3). Expression of six of these proteins increased in abundance at both 5 and 20 min post-treatment, while six decreased after either ABA or H₂O₂ treatment (Table 3). The other nine proteins showed dissimilar regulation patterns between the two treatments.

Table 3. Comparison differential protein accumulation in response to ABA and H₂O₂.

Accession Number	Protein Name	H ₂ O ₂ 5 min	H ₂ O ₂ 20 min	ABA 5 min	ABA 20 min
1. Metabolism					
AT1G17745	D-3-phosphoglycerate dehydrogenase 2	0.1	0.1	0.1	0.2
AT5G17770	NADH:cytochrome B5 reductase 1	0.4	2.5	2.3	2.3
2. Energy					
AT2G05710	Aconitase 3	2.5	12	8	9.9
AT1G15120	Ubiquinol-cytochrome C reductase hinge	19	20	15	11
3. Transcription					
AT1G14850	Nucleoporin 155	ns	0.3	0.1	0.2
4. Protein synthesis					
AT3G04400	Ribosomal protein L14p/L23e	3.8	3	3.5	2.6
AT3G45030	Ribosomal protein S10p/S20e	ns	2.2	2.3	ns
AT1G01100	60S acidic ribosomal protein family	ns	0.4	0.4	0.4
5. Protein destination and storage					
AT1G14980	Chaperonin 10	ns	2.9	2.5	3
AT5G56030	Heat shock protein 81-2	0.4	ns	0.4	0.5
6. Transporters					
AT4G27500	Proton pump interactor 1	ns	2.4	ns	2.3
AT3G08530	Clathrin, heavy chain	0.5	0.2	0.2	0.4
AT3G11130	Clathrin, heavy chain	0.5	0.4	0.3	0.4
7. Intracellular traffic					
AT1G61570	Mit. import inner membrane 13 translocase	17	23	19	11
8. Cell structure					
AT5G09810	Actin 7	0.5	ns	0.5	0.5
AT4G14960	Tubulin/FtsZ family protein	0.4	0.5	0.4	0.3
AT5G62690	Tubulin beta chain 2	0.4	0.4	0.3	0.4
AT2G29550	Tubulin beta-7 chain	0.3	0.4	0.3	0.4
AT5G19770	Tubulin alpha-3	0.1	ns	0.5	0.3
9. Signal transduction					
AT3G51800	Metallopeptidase M24 family protein	5.1	ns	3.4	ns
AT3G14840	LRR transmembrane protein kinase	ns	11	8.3	14

Three proteins, ubiquinol-cytochrome C reductase hinge (UQCRH, AT1G15120), D-3-phosphoglycerate dehydrogenase (AT1G17745) and NADH:cytochrome B5 reductase 1 (Cytb5R, AT5G17770), belonging to the molecular function category 'oxidoreductase activity' (Table S2), showed differential accumulation in response to either ABA or H₂O₂ (Table 3). Oxidoreductase-related proteins have been shown to control responses to calcium homeostasis in organelles such as endoplasmic reticulum [58]. Besides, amongst the identified ABA and H₂O₂-responsive proteins, UQCRH was one of the proteins increasing in abundance the most at both time points. It is a component of the mitochondrial respiratory chain complex III. Cytb5R is an integral membrane-bound flavoprotein that is localised mainly in the endoplasmic reticulum and the outer mitochondrial membrane [59]. It is an electron donor for Cytb5, a membrane-haeme-containing protein [60]. Non-cytotoxic concentration of H₂O₂ (24 µM) has been shown to induce a significant up-regulation of Cytb5R, suggesting a redox regulation [61]. However, in this study, we observed that a higher concentration of H₂O₂ (50 µM) can cause a decrease of Cytb5R abundance as an early response, and an increase at 20 min. This may suggest concentration-dependent redox regulation by Cytb5R in response H₂O₂ as well as ABA.

Within the common proteins set, the most represented functional category was the cell structure, comprising of four tubulins and one actin. Tubulin/FtsZ protein (AT4G14960), an α-tubulin isoform that is required for right handed helical growth, is part of the tubulin complex or structural constituent of the cytoskeleton [62]. Tubulins showed differential expression in response to salt stress, for example, abundance of tubulin β-chain 2 (AT5G62690) decreased after salt treatment [63]. Tubulin has also been shown to regulate low nitrate-induced anthocyanin biosynthesis and plant nitrate response regulatory network in collaboration with other signalling pathways including ABA and H₂O₂ [64]. The four tubulins and actin 7 identified in the current study were all down-regulated in response to ABA and H₂O₂, and showed reduction in transcriptional level during senescence suggesting that the cytoskeletal

organization-related proteins are affected by oxidative stress. Further, the cytoskeleton has been shown to be essential for mitochondrial morphology, movement and immobilization. The actin cytoskeleton, for example, is involved in the immobilization of mitochondria at the cortex in cultured tobacco cells, and the cytoskeleton may be critical for retaining mitochondria at sites of high ATP demand (for review see [65]).

To further examine the mutual effect of ABA and H₂O₂, in particular to shed light on the common protein cohort whether the ABA effect is a result of the H₂O₂ signalling initiated via ABA pathway, we performed an ABA assay following H₂O₂ treatment of Arabidopsis cell suspension cultures and vice-versa. We noted no significant change in ABA quantity at 5 and 20 min post-H₂O₂ treatment. This may be attributed to the short treatment times aimed at observing early stimuli responses, or potentially from the low concentration of H₂O₂ used. Previously, it has been revealed that treating Arabidopsis guard cells with 100 µM H₂O₂ for 25 and 30 min induced an ABA-mediated nitric oxide production, which in turn is dependent on ABA-induced H₂O₂ synthesis [66]. Furthermore, a ROS assay was performed after treating Arabidopsis cell suspension cultures with 50 µM ABA. Here, we observed an increase in ROS accumulation at 20 min when compared with the controls (collected at 0 and 20 min) (Figure 2). This observation is not new as previously, ABA has been shown to induce H₂O₂ production through NADPH oxidase [67] and in guard cells of *Vicia faba*, ABA was also observed to generate H₂O₂ [68]. Additionally, in Arabidopsis, ROS accumulation was noted to occur upon ABA-induced stomatal closure [69]. Therefore, this suggests that ABA directly and/or indirectly induce ROS production in the cells that may lead to the observed common regulation of downstream processes with H₂O₂.

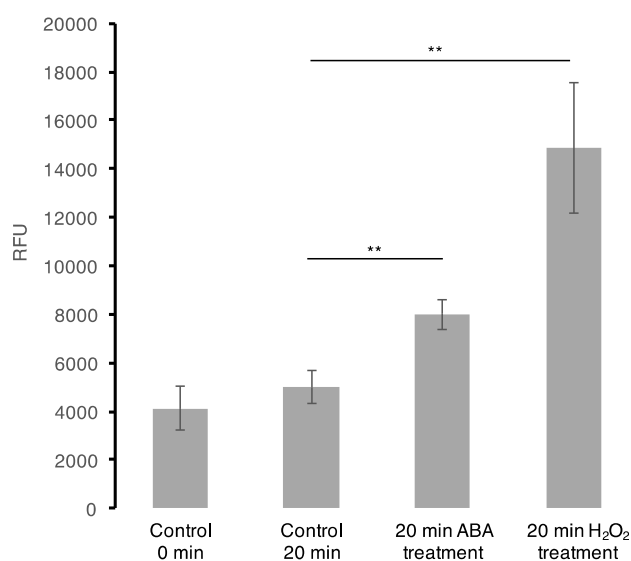


Figure 2. Reactive oxygen species (ROS) assay. OxiSelect™ Intracellular ROS assay kit (Cell Biolabs, Inc., San Diego, CA, USA) was used in the in vivo oxidation experiments using cultured Arabidopsis (Col-0) cells according to the assay protocol provided by the manufacturer. Each bar represents data from four biological replicates ($n = 4$) with a calculated standard error. Treatment of cells with ABA at the final concentration of 50 µM induces a statistically significant increase in H₂O₂ production, $p < 0.001$ (represented by two asterisks (**)) symbols) using a two-sample t -test.

4. Conclusions

Shotgun proteomics approaches can distinguish common and specific responses linked to ABA or H₂O₂ treatments. The analysed proteomics data also revealed over 30 microsomal proteins associated with RNA interaction [70]. Furthermore, amongst the common set of proteins, we detected three proteins, namely aconitase 3, UQCRH, and inner mitochondrial membrane translocase 13, to be the

most responsive and potentially as promising signatures for both ABA and H₂O₂ although they require further investigation to determine their mode of action. Besides, the fact that most of the common proteins changed in abundance in a similar manner is consistent with ABA-induced ROS production. Finally, we also show that a significant protein subset responds specifically to either ABA or H₂O₂, suggesting that these molecules also modulate independent complex intracellular responses.

Supplementary Materials: The following are available online <http://www.mdpi.com/2227-7382/5/3/22/s1>, Table S2: H₂O₂ differentially expressed proteins and GO analysis, Table S3: ABA differentially expressed proteins and GO analysis.

Acknowledgments: The authors would like to thank Bothayna Algashgari for technical assistance. The mass spectrometry proteomics data have been deposited to the ProteomeXchange Consortium via the PRIDE [71] partner repository with the dataset identifier PXD006513.

Author Contributions: C.M. and C.G. conceived and designed the experiments; M.A. and L.T. performed the experiments; C.M., M.A. and L.T. analysed the data; C.M. wrote the paper; C.M. and C.G. critically revised the manuscript.

Conflicts of Interest: The authors declare no conflict of interest.

References

1. Dat, J.; Vandenabeele, S.; Vranova, E.; Van Montagu, M.; Inze, D.; Van Breusegem, F. Dual action of the active oxygen species during plant stress responses. *Cell Mol. Life Sci.* **2000**, *57*, 779–795. [[CrossRef](#)] [[PubMed](#)]
2. Luna, C.M.; Pastori, G.M.; Driscoll, S.; Groten, K.; Bernard, S.; Foyer, C.H. Drought controls on H₂O₂ accumulation, catalase (CAT) activity and CAT gene expression in wheat. *J. Exp. Bot.* **2005**, *56*, 417–423. [[CrossRef](#)] [[PubMed](#)]
3. Zhang, F.; Wang, Y.; Yang, Y.; Wu, H.; Wang, D.; Liu, J. Involvement of hydrogen peroxide and nitric oxide in salt resistance in the calluses from *Populus euphratica*. *Plant Cell Environ.* **2007**, *30*, 775–785. [[CrossRef](#)] [[PubMed](#)]
4. Mittler, R.; Herr, E.H.; Orvar, B.L.; van Camp, W.; Willekens, H.; Inze, D.; Ellis, B.E. Transgenic tobacco plants with reduced capability to detoxify reactive oxygen intermediates are hyperresponsive to pathogen infection. *Proc. Natl. Acad. Sci. USA* **1999**, *96*, 14165–14170. [[CrossRef](#)] [[PubMed](#)]
5. Halliwell, B. Free radicals, reactive oxygen species and human disease: A critical evaluation with special reference to atherosclerosis. *Br. J. Exp. Pathol.* **1989**, *70*, 737–757. [[PubMed](#)]
6. Moller, I.M. Plant mitochondria and oxidative stress: Electron transport, NADPH turnover, and metabolism of reactive oxygen species. *Annu. Rev. Plant Physiol. Plant Mol. Biol.* **2001**, *52*, 561–591. [[CrossRef](#)] [[PubMed](#)]
7. Millar, H.; Considine, M.J.; Day, D.A.; Whelan, J. Unraveling the role of mitochondria during oxidative stress in plants. *IUBMB Life* **2001**, *51*, 201–205. [[PubMed](#)]
8. Schmidtman, E.; Konig, A.C.; Orwat, A.; Leister, D.; Hartl, M.; Finkemeier, I. Redox regulation of Arabidopsis mitochondrial citrate synthase. *Mol. Plant* **2014**, *7*, 156–169. [[CrossRef](#)] [[PubMed](#)]
9. Verniquet, F.; Gaillard, J.; Neuburger, M.; Douce, R. Rapid inactivation of plant aconitase by hydrogen peroxide. *Biochem. J.* **1991**, *276*, 643–648. [[CrossRef](#)] [[PubMed](#)]
10. Millar, A.H.; Leaver, C.J. The cytotoxic lipid peroxidation product, 4-hydroxy-2-nonenal, specifically inhibits decarboxylating dehydrogenases in the matrix of plant mitochondria. *FEBS Lett.* **2000**, *481*, 117–121. [[CrossRef](#)]
11. Sweetlove, L.J.; Heazlewood, J.L.; Herald, V.; Holtzapffel, R.; Day, D.A.; Leaver, C.J.; Millar, A.H. The impact of oxidative stress on Arabidopsis mitochondria. *Plant J.* **2002**, *32*, 891–904. [[CrossRef](#)] [[PubMed](#)]
12. Desikan, R.; Reynolds, A.; Hancock, J.T.; Neill, S.J. Harpin and hydrogen peroxide both initiate programmed cell death but have differential effects on defence gene expression in Arabidopsis suspension cultures. *Biochem. J.* **1998**, *330*, 115–120. [[CrossRef](#)] [[PubMed](#)]
13. Pei, Z.M.; Murata, Y.; Benning, G.; Thomine, S.; Klusener, B.; Allen, G.J.; Grill, E.; Schroeder, J.I. Calcium channels activated by hydrogen peroxide mediate abscisic acid signaling in guard cells. *Nature* **2000**, *406*, 731–734. [[CrossRef](#)] [[PubMed](#)]
14. Kwak, J.M.; Mori, I.C.; Pei, Z.M.; Leonhardt, N.; Torres, M.A.; Dangel, J.L.; Bloom, R.E.; Bodde, S.; Jones, J.D.G.; Schroeder, J.I. NADPH oxidase AtrbohD and AtrbohF genes function in ROS-dependent ABA signaling in Arabidopsis. *EMBO J.* **2003**, *22*, 2623–2633. [[CrossRef](#)] [[PubMed](#)]

15. Guan, L.M.; Zhao, J.; Scandalios, J.G. Cis-elements and trans-factors that regulate expression of the maize *Cat1* antioxidant gene in response to ABA and osmotic stress: H₂O₂ is the likely intermediary signaling molecule for the response. *Plant J.* **2000**, *22*, 87–95. [CrossRef] [PubMed]
16. Gonzalez-Guzman, M.; Pizzio, G.A.; Antoni, R.; Vera-Sirera, F.; Merilo, E.; Bassel, G.W.; Fernandez, M.A.; Holdsworth, M.J.; Perez-Amador, M.A.; Kollist, H.; et al. Arabidopsis PYR/PYL/RCAR receptors play a major role in quantitative regulation of stomatal aperture and transcriptional response to abscisic acid. *Plant Cell* **2012**, *24*, 2483–2496. [CrossRef] [PubMed]
17. Joshi-Saha, A.; Valon, C.; Leung, J. A brand new START: Abscisic acid perception and transduction in the guard cell. *Sci. Signal.* **2011**, *4*, re4. [CrossRef] [PubMed]
18. Arve, L.E.; Carvalho, D.R.; Olsen, J.E.; Torre, S. ABA induces H₂O₂ production in guard cells, but does not close the stomata on *Vicia faba* leaves developed at high air humidity. *Plant Signal. Behav.* **2014**, *9*, e29192. [CrossRef] [PubMed]
19. Desikan, R.; Cheung, M.K.; Bright, J.; Henson, D.; Hancock, J.T.; Neill, S.J. ABA, hydrogen peroxide and nitric oxide signaling in stomatal guard cells. *J. Exp. Bot.* **2004**, *55*, 205–212. [CrossRef] [PubMed]
20. Murata, Y.; Pei, Z.M.; Mori, I.C.; Schroeder, J. Abscisic acid activation of plasma membrane Ca²⁺ channels in guard cells requires cytosolic NAD(P)H and is differentially disrupted upstream and downstream of reactive oxygen species production in *abi1-1* and *abi2-1* protein phosphatase 2C mutants. *Plant Cell* **2001**, *13*, 2513–2523. [CrossRef] [PubMed]
21. Giraudat, J.; Parcy, F.; Bertauche, N.; Gosti, F.; Leung, J.; Morris, P.C.; Bouvier-Durand, M.; Vartanian, N. Current advances in abscisic acid action and signaling. *Plant Mol. Biol.* **1994**, *26*, 1557–1577. [CrossRef] [PubMed]
22. Yang, L.; Zhang, J.; He, J.; Qin, Y.; Hua, D.; Duan, Y.; Chen, Z.; Gong, Z. ABA-mediated ROS in mitochondria regulate root meristem activity by controlling PLETHORA expression in Arabidopsis. *PLoS Genet.* **2014**, *10*, e1004791. [CrossRef] [PubMed]
23. Hu, X.; Zhang, A.; Zhang, J.; Jiang, M. Abscisic acid is a key inducer of hydrogen peroxide production in leaves of maize plants exposed to water stress. *Plant Cell Physiol.* **2006**, *47*, 1484–1495. [CrossRef] [PubMed]
24. Jiang, M.; Zhang, J. Involvement of plasma-membrane NADPH oxidase in abscisic acid- and water stress-induced antioxidant defense in leaves of maize seedlings. *Planta* **2002**, *215*, 1022–1030. [CrossRef] [PubMed]
25. Liu, C.-H.; Chao, Y.-Y.; Kao, C.H. Abscisic acid is an inducer of hydrogen peroxide production in leaves of rice seedlings grown under potassium deficiency. *Bot. Stud.* **2012**, *53*, 229–237.
26. Marondedze, C.; Turek, I.; Parrott, B.; Thomas, L.; Jankovic, B.; Lilley, K.S.; Gehring, C. Structural and functional characteristics of cGMP-dependent methionine oxidation in *Arabidopsis thaliana* proteins. *Cell Commun. Signal.* **2013**, *11*. [CrossRef] [PubMed]
27. Marondedze, C.; Wong, A.; Groen, A.; Serrano, N.; Jankovic, B.; Lilley, K.; Gehring, C.; Thomas, L. Exploring the Arabidopsis proteome: Influence of protein solubilization buffers on proteome coverage. *Int. J. Mol. Sci.* **2015**, *16*, 857–870. [CrossRef] [PubMed]
28. Ordonez, N.M.; Marondedze, C.; Thomas, L.; Pasqualini, S.; Shabala, L.; Shabala, S.; Gehring, C. Cyclic mononucleotides modulate potassium and calcium flux responses to H₂O₂ in Arabidopsis roots. *FEBS Lett.* **2014**, *588*, 1008–1015. [CrossRef] [PubMed]
29. Thomas, L.; Marondedze, C.; Ederli, L.; Pasqualini, S.; Gehring, C. Proteomic signatures implicate cAMP in light and temperature responses in *Arabidopsis thaliana*. *J. Proteom.* **2013**, *83*, 47–59. [CrossRef] [PubMed]
30. Groen, A.; Thomas, L.; Lilley, K.; Marondedze, C. Identification and quantitation of signal molecule-dependent protein phosphorylation. *Methods Mol. Biol.* **2013**, *1016*, 121–137. [PubMed]
31. Bevan, M.; Bancroft, I.; Bent, E.; Love, K.; Goodman, H.; Dean, C.; Bergkamp, R.; Dirkse, W.; van Staveren, M.; Stiekema, W.; et al. Analysis of 1.9 Mb of contiguous sequence from chromosome 4 of *Arabidopsis thaliana*. *Nature* **1998**, *391*, 485–488. [CrossRef] [PubMed]
32. AgriGO. Available online: <http://bioinfo.cau.edu.cn/agriGO/> (accessed on 1 February 2017).
33. Moreno-Sanchez, R.; Saavedra, E.; Rodriguez-Enriquez, S.; Gallardo-Perez, J.C.; Quezada, H.; Westerhoff, H.V. Metabolic control analysis indicates a change of strategy in the treatment of cancer. *Mitochondrion* **2010**, *10*, 626–639. [CrossRef] [PubMed]

34. Araujo, W.L.; Nunes-Nesi, A.; Nikoloski, Z.; Sweetlove, L.J.; Fernie, A.R. Metabolic control and regulation of the tricarboxylic acid cycle in photosynthetic and heterotrophic plant tissues. *Plant Cell Environ.* **2012**, *35*, 1–21. [[CrossRef](#)] [[PubMed](#)]
35. Tretter, L.; Adam-Vizi, V. Alpha-ketoglutarate dehydrogenase: A target and generator of oxidative stress. *Philos. Trans. R. Soc. Lond. Biol. Sci.* **2005**, *360*, 2335–2345. [[CrossRef](#)] [[PubMed](#)]
36. Janero, D.R.; Hreniuk, D. Suppression of TCA cycle activity in the cardiac muscle cell by hydroperoxide-induced oxidant stress. *Am. J. Physiol.* **1996**, *270*, C1735–C1742. [[PubMed](#)]
37. Moeder, W.; Del Pozo, O.; Navarre, D.A.; Martin, G.B.; Klessig, D.F. Aconitase plays a role in regulating resistance to oxidative stress and cell death in *Arabidopsis* and *Nicotiana benthamiana*. *Plant Mol. Biol.* **2007**, *63*, 273–287. [[CrossRef](#)] [[PubMed](#)]
38. Hentze, M.W.; Argos, P. Homology between IRE-BP, a regulatory RNA-binding protein, aconitase, and isopropylmalate isomerase. *Nucleic Acids Res.* **1991**, *19*, 1739–1740. [[CrossRef](#)] [[PubMed](#)]
39. Marondedze, C.; Thomas, L.; Serrano, N.L.; Lilley, K.S.; Gehring, C. The RNA-binding protein repertoire of *Arabidopsis thaliana*. *Sci. Rep.* **2016**, *6*, 29766. [[CrossRef](#)] [[PubMed](#)]
40. Heyndrickx, K.S.; Vandepoele, K. Systematic identification of functional plant modules through the integration of complementary data sources. *Plant Physiol.* **2012**, *159*, 884–901. [[CrossRef](#)] [[PubMed](#)]
41. Martiniere, A.; Li, X.; Runions, J.; Lin, J.; Maurel, C.; Luu, D.T. Salt stress triggers enhanced cycling of *Arabidopsis* root plasma-membrane aquaporins. *Plant Signal. Behav.* **2012**, *7*, 529–532. [[CrossRef](#)] [[PubMed](#)]
42. Niittyta, T.; Fuglsang, A.T.; Palmgren, M.G.; Frommer, W.B.; Schulze, W.X. Temporal analysis of sucrose-induced phosphorylation changes in plasma membrane proteins of *Arabidopsis*. *Mol. Cell Proteom.* **2007**, *6*, 1711–1726. [[CrossRef](#)] [[PubMed](#)]
43. Kammerloher, W.; Fischer, U.; Piechotka, G.P.; Schaffner, A.R. Water channels in the plant plasma membrane cloned by immunoselection from a mammalian expression system. *Plant J.* **1994**, *6*, 187–199. [[CrossRef](#)] [[PubMed](#)]
44. Dynowski, M.; Schaaf, G.; Loque, D.; Moran, O.; Ludewig, U. Plant plasma membrane water channels conduct the signaling molecule H₂O₂. *Biochem. J.* **2008**, *414*, 53–61. [[CrossRef](#)] [[PubMed](#)]
45. Wudick, M.M.; Li, X.; Valentini, V.; Geldner, N.; Chory, J.; Lin, J.; Maurel, C.; Luu, D.T. Subcellular redistribution of root aquaporins induced by hydrogen peroxide. *Mol. Plant* **2015**, *8*, 1103–1114. [[CrossRef](#)] [[PubMed](#)]
46. Kline, K.G.; Barrett-Wilt, G.A.; Sussman, M.R. In planta changes in protein phosphorylation induced by the plant hormone abscisic acid. *Proc. Natl. Acad. Sci. USA* **2010**, *107*, 15986–15991. [[CrossRef](#)] [[PubMed](#)]
47. Grondin, A.; Rodrigues, O.; Verdoucq, L.; Merlot, S.; Leonhardt, N.; Maurel, C. Aquaporins contribute to ABA-Triggered stomatal closure through OST1-mediated phosphorylation. *Plant Cell* **2015**, *27*, 1945–1954. [[CrossRef](#)] [[PubMed](#)]
48. Hwang, I.S.; Hwang, B.K. The pepper mannose-binding lectin gene CaMBL1 is required to regulate cell death and defense responses to microbial pathogens. *Plant Physiol.* **2011**, *155*, 447–463. [[CrossRef](#)] [[PubMed](#)]
49. Leonhardt, N.; Kwak, J.M.; Robert, N.; Waner, D.; Leonhardt, G.; Schroeder, J.I. Microarray expression analyses of *Arabidopsis* guard cells and isolation of a recessive abscisic acid hypersensitive protein phosphatase 2C mutant. *Plant Cell* **2004**, *16*, 596–615. [[CrossRef](#)] [[PubMed](#)]
50. Zhang, W.L.; Peumans, W.J.; Barre, A.; Astoul, C.H.; Rovira, P.; Rouge, P.; Proost, P.; Truffa-Bachi, P.; Jalali, A.A.H.; Van Damme, E.J.M. Isolation and characterization of a jacalin-related mannose-binding lectin from salt-stressed rice (*Oryza sativa*) plants. *Planta* **2000**, *210*, 970–978. [[PubMed](#)]
51. Feng, H.; Xu, W.Z.; Lin, H.H.; Chong, K. Transcriptional regulation of wheat VER2 promoter in rice in response to abscisic acid, jasmonate, and light. *J. Genet. Genom.* **2009**, *36*, 371–377. [[CrossRef](#)]
52. Fouquaert, E.; Van Damme, E.J. Promiscuity of the euonymus carbohydrate-binding domain. *Biomolecules* **2012**, *2*, 415–434. [[CrossRef](#)] [[PubMed](#)]
53. Song, M.; Xu, W.Q.; Xiang, Y.; Jia, H.Y.; Zhang, L.X.; Ma, Z.Q. Association of jacalin-related lectins with wheat responses to stresses revealed by transcriptional profiling. *Plant Mol. Biol.* **2014**, *84*, 95–110. [[CrossRef](#)] [[PubMed](#)]
54. Le, M.H.; Cao, Y.; Zhang, X.C.; Stacey, G. LIK1, a CERK1-interacting kinase, regulates plant immune responses in *Arabidopsis*. *PLoS ONE* **2014**, *9*, e102245. [[CrossRef](#)] [[PubMed](#)]

55. Wan, J.; Zhang, X.C.; Neece, D.; Ramonell, K.M.; Clough, S.; Kim, S.Y.; Stacey, M.G.; Stacey, G. A LysM receptor-like kinase plays a critical role in chitin signaling and fungal resistance in Arabidopsis. *Plant Cell* **2008**, *20*, 471–481. [[CrossRef](#)] [[PubMed](#)]
56. Miya, A.; Albert, P.; Shinya, T.; Desaki, Y.; Ichimura, K.; Shirasu, K.; Narusaka, Y.; Kawakami, N.; Kaku, H.; Shibuya, N. CERK1, a LysM receptor kinase, is essential for chitin elicitor signaling in Arabidopsis. *Proc. Natl. Acad. Sci. USA* **2007**, *104*, 19613–19618. [[CrossRef](#)] [[PubMed](#)]
57. Williams, B.; Kabbage, M.; Kim, H.J.; Britt, R.; Dickman, M.B. Tipping the balance: Sclerotinia sclerotiorum secreted oxalic acid suppresses host defenses by manipulating the host redox environment. *PLoS Pathog.* **2011**, *7*, e1002107. [[CrossRef](#)] [[PubMed](#)]
58. Groenendyk, J.; Peng, Z.; Dudek, E.; Fan, X.; Mizianty, M.J.; Dufey, E.; Urra, H.; Sepulveda, D.; Rojas-Rivera, D.; Lim, Y.; et al. Interplay between the oxidoreductase PDIA6 and microRNA-322 controls the response to disrupted endoplasmic reticulum calcium homeostasis. *Sci. Signal.* **2014**, *7*, ra54. [[CrossRef](#)] [[PubMed](#)]
59. Borgese, N.; Aggujaro, D.; Carrera, P.; Pietrini, G.; Bassetti, M. A role for N-myristoylation in protein targeting: NADH-cytochrome b5 reductase requires myristic acid for association with outer mitochondrial but not ER membranes. *J. Cell Biol.* **1996**, *135*, 1501–1513. [[CrossRef](#)] [[PubMed](#)]
60. Fukuchi-Mizutani, M.; Mizutani, M.; Tanaka, Y.; Kusumi, T.; Ohta, D. Microsomal electron transfer in higher plants: cloning and heterologous expression of NADH-cytochrome b5 reductase from Arabidopsis. *Plant Physiol.* **1999**, *119*, 353–362. [[CrossRef](#)] [[PubMed](#)]
61. Bello, R.I.; Alcain, F.J.; Gomez-Diaz, C.; Lopez-Lluch, G.; Navas, P.; Villalba, J.M. Hydrogen peroxide- and cell-density-regulated expression of NADH-cytochrome b5 reductase in HeLa cells. *J. Bioenerg. Biomembr.* **2003**, *35*, 169–179. [[CrossRef](#)] [[PubMed](#)]
62. Abe, T.; Hashimoto, T. Altered microtubule dynamics by expression of modified alpha-tubulin protein causes right-handed helical growth in transgenic Arabidopsis plants. *Plant J.* **2005**, *43*, 191–204. [[CrossRef](#)] [[PubMed](#)]
63. Jiang, Y.; Yang, B.; Harris, N.S.; Deyholos, M.K. Comparative proteomic analysis of NaCl stress-responsive proteins in Arabidopsis roots. *J. Exp. Bot.* **2007**, *58*, 3591–3607. [[CrossRef](#)] [[PubMed](#)]
64. Wang, X.; Bian, Y.; Cheng, K.; Zou, H.; Sun, S.S.; He, J.X. A comprehensive differential proteomic study of nitrate deprivation in Arabidopsis reveals complex regulatory networks of plant nitrogen responses. *J. Proteom. Res.* **2012**, *11*, 2301–2315. [[CrossRef](#)] [[PubMed](#)]
65. Boldogh, I.R.; Pon, L.A. Interactions of mitochondria with the actin cytoskeleton. *Biochim. Biophys. Acta* **2006**, *1763*, 450–462. [[CrossRef](#)] [[PubMed](#)]
66. Bright, J.; Desikan, R.; Hancock, J.T.; Weir, I.S.; Neill, S.J. ABA-induced NO generation and stomatal closure in Arabidopsis are dependent on H₂O₂ synthesis. *Plant J.* **2006**, *45*, 113–122. [[CrossRef](#)] [[PubMed](#)]
67. Foreman, J.; Demidchik, V.; Bothwell, J.H.; Mylona, P.; Miedema, H.; Torres, M.A.; Linstead, P.; Costa, S.; Brownlee, C.; Jones, J.D.; et al. Reactive oxygen species produced by NADPH oxidase regulate plant cell growth. *Nature* **2003**, *422*, 442–446. [[CrossRef](#)] [[PubMed](#)]
68. Zhang, X.; Zhang, L.; Dong, F.; Gao, J.; Galbraith, D.W.; Song, C.P. Hydrogen peroxide is involved in abscisic acid-induced stomatal closure in *Vicia faba*. *Plant Physiol.* **2001**, *126*, 1438–1448. [[CrossRef](#)] [[PubMed](#)]
69. Penson, S.P.; Schuurink, R.C.; Fath, A.; Gubler, F.; Jacobsen, J.V.; Jones, R.L. cGMP is required for gibberellic acid-induced gene expression in barley aleurone. *Plant Cell* **1996**, *8*, 2325–2333. [[CrossRef](#)] [[PubMed](#)]
70. Marondedze, C.; Groen, A.J.; Thomas, L.; Lilley, K.S.; Gehring, C. A Quantitative phosphoproteome analysis of cGMP-dependent cellular responses in *Arabidopsis thaliana*. *Mol. Plant* **2016**, *9*, 621–623. [[CrossRef](#)] [[PubMed](#)]
71. Vizcaíno, J.A.; Csordas, A.; Del-Toro, N.; Dianes, J.A.; Griss, J.; Lavidas, I.; Mayer, G.; Perez-Riverol, Y.; Reisinger, F.; Ternent, T.; et al. 2016 update of the PRIDE database and related tools. *Nucleic Acids Res.* **2016**, *44*, D447–D456. [[CrossRef](#)] [[PubMed](#)]

